REPORT DOCUMENTATION PAGE

Form Approved
OMB No. 0704-0188

1. REPORT DATE *(DD-MM-YYYY)*	2. REPORT TYPE	3. DATES COVERED *(From - To)*
	Technical Papers	

4. TITLE AND SUBTITLE

Please see attached

5a. CONTRACT NUMBER

5b. GRANT NUMBER

5c. PROGRAM ELEMENT NUMBER

6. AUTHOR(S)

5d. PROJECT NUMBER
1011

5e. TASK NUMBER
0046

5f. WORK UNIT NUMBER
346204

7. PERFORMING ORGANIZATION NAME(S) AND ADDRESS(ES)

Air Force Research Laboratory (AFMC)
AFRL/PRS
5 Pollux Drive
Edwards AFB CA 93524-7048

8. PERFORMING ORGANIZATION REPORT

9. SPONSORING / MONITORING AGENCY NAME(S) AND ADDRESS(ES)

Air Force Research Laboratory (AFMC)
AFRL/PRS
5 Pollux Drive
Edwards AFB CA 93524-7048

10. SPONSOR/MONITOR'S ACRONYM(S)

11. SPONSOR/MONITOR'S NUMBER(S)
Please see attached

12. DISTRIBUTION / AVAILABILITY STATEMENT

Approved for public release; distribution unlimited.

13. SUPPLEMENTARY NOTES

14. ABSTRACT

15. SUBJECT TERMS

16. SECURITY CLASSIFICATION OF:			17. LIMITATION OF ABSTRACT	18. NUMBER OF PAGES	19a. NAME OF RESPONSIBLE PERSON
a. REPORT	b. ABSTRACT	c. THIS PAGE			Leilani Richardson
Unclassified	Unclassified	Unclassified	A		19b. TELEPHONE NUMBER *(include area code)* (661) 275-5015

[redacted]

MEMORANDUM FOR PRS (In-House Publication)

FROM: PROI (TI) (STINFO) 5429

03 Jan 2001

SUBJECT: Authorization for Release of Technical Information, Control Number: **AFRL-PR-ED-TP-2001-003**
Larson, C.W.; Mead, F.B., "Energy Conversion in Laser Propulsion"

39th AIAA Aerospace Sciences Meeting and Exhibit **(Statement A)**
(Reno, NV, 8-11 Jan 2001) (Deadline: 05 Jan 2001)

AIAA 2001-0646
Energy Conversion in Laser Propulsion

C. W. Larson and F. B. Mead, Jr.
Air Force Research Laboratory
Edwards AFB, CA 93524

39th AIAA Aerospace Sciences Meeting & Exhibit
8-11 January 2001 / Reno, NV

Energy Conversion in Laser propulsion

C. William Larson and Franklin B. Mead, Jr.
Propulsion Directorate
Air Force Research Laboratory
Edwards AFB, CA 93524-7680

Abstract

Analysis of energy conversion in laser propulsion is reported and compared to experimental studies of a laboratory scale propulsion device that absorbs laser energy and converts that energy to propellant kinetic energy. The propellants studied were air and Delrin, a solid with the composition of formaldehyde [H_2CO] that vaporizes cleanly upon laser irradiation. The Myrabo Laser Lightcraft (MLL) was studied. It incorporates an inverted parabolic reflector that focuses laser energy into a toroidal volume where it is absorbed by a unit of propellant mass that is subsequently expanded in the geometry of the plug nozzle aerospike. The results showed that between 30 and 50% of the incident laser energy is converted to propellant kinetic energy. This overall absorption/expansion efficiency was examined in terms of the thermodynamic predictions of conversion of propellant internal energy to propellant kinetic energy. Expansion of a propellant mass that was heated at constant volume was examined under conditions where either chemical equilibrium or frozen composition was maintained. For expansion with an effective area ratio of ~ 4, which is appropriate for the MLL, a maximum of 25 to 50% of the internal energy is predicted to be convertible to propellant kinetic energy, based on the minimization of the entropy gain of the blowdown process. With the small effective area ratio ~ 4, equilibrium expansion was only slightly more efficient than frozen expansion. Heating of propellant to highly ionized states resulted in lower efficiency energy conversion but higher exit velocity. The thermodynamic limitations are illustrated by process representations of blowdown in the Mollier plane (enthalpy vs entropy diagram for air). The analysis captures the equation of state of the partially ionized propellant under conditions of chemical equilibrium.

Nomenclature (in order of use)

$\mathbf{F}$	Force or thrust, N = kg m/s^2.
m	mass of rocket, kg.
t	time, s
$\mathbf{v_e}$	exit velocity of propellant relative to the rocket, in the rocket frame of reference, m/s.
dm/dt	incremental mass change of rocket, instantaneous propellant mass flow rate, kg/s.
dv/dt	incremental velocity change of rocket in the inertial frame of reference, m/s^2.
v_i	initial velocity of rocket in inertial frame, m/s.
v_f	final velocity of rocket in inertial frame, m/s
m_i	initial mass of rocket, kg.
m_f	final mass of rocket, kg.
m_i-m_f	mass of propellant, kg.
f	mass fraction for a rocket mission, $f = m_f/m_i$.
x	ratio of $v_f - v_i$ to v_e.
y	ratio of v_i to v_e.
η_1	mass efficiency of mission = mass of vehicle/mass of propellant.
η_2	momentum efficiency of mission = momentum change of vehicle/momentum of propellant.
η_3	energy efficiency of mission = kinetic energy change of mission/kinetic energy of propellant.
C_1	mass coupling coefficient = mass of vehicle/kinetic energy of propellant.
$\mathbf{C_2}$	momentum coupling coefficient = momentum change of vehicle/kinetic energy of propellant.
C_3	energy coupling coefficient = kinetic energy change of vehicle/kinetic energy of propellant.
K_1	mass cost function = kinetic energy of propellant/mass of vehicle
$\mathbf{K_2}$	momentum cost function = kinetic energy of propellant/momentum change of vehicle.
K_3	energy cost function = kinetic energy of propellant/kinetic energy change of vehicle.
η_{Sutton}	Sutton's "propulsive efficiency", $\eta_{Sutton} = y^2/(1-y^2)$.
M	mass of Laser Lightcraft, kg.

h	altitude achieved in laser powered flight, m.
g	acceleration of gravity, 9.806 m/s^2.
E_L	laser energy incident on propellant per pulse, J/pulse.
ω	frequency of laser, pulse/s.
T/W	thrust to weight ratio, $T/W = C_2 E_L \omega / Mg$.
P_L	power of laser, J/s, $P_L = \omega E_L$.
α	efficiency of conversion of propellant internal energy to propellant kinetic energy.
β	fraction of incident laser energy absorbed by propellant.
I	impulse, Ns = kg m/s.
$\mathbf{C_2(exp)}$	experimental momentum coupling coefficient, Ns/J = s/m.
m_{pen}	total mass of pendulum and test article, kg.
l	distance between pendulum pivot and center of gravity, m.
θ	angle of deflection of pendulum, degrees.
$\mathbf{I_{hammer}}$	Standard impulse imparted to pendulum by NBS traceable hammer accelerometer, Ns
$\mathbf{I_{pendulum}}$	Impulse measured with ballistic pendulum, Ns.
m_D	mass of Delrin ablated in a single laser shot, kg.
u	specific internal energy of laser heated propellant, J/kg.
u_e	specific internal energy of propellant at the exit of the rocket after isentropic expansion.

Introduction

Analysis of the limitations of laser propulsion and optimization of the mission parameters that are imposed by Newton's second law was published independently and nearly simultaneously 25 years ago by Moeckel (1975) and Lo (1976). Phipps, Reilly and Campbell (2000, 2001) recently cited Moeckel's paper in their comprehensive analysis of the Earth to LEO mission powered by laser propulsion. Here we show the elementary relationships between the mission parameters and three mission efficiencies, the mass, momentum and energy efficiency, and their associated coupling coefficients and cost functions. The efficiency of conversion of laser energy to propellant kinetic energy, based on various ballistic pendulum and flight experiments with Myrabo Laser Lightcraft, MLL [Messitt, Myrabo, and Mead (2000); Mead, Squires, Beairsto, and Thurston (2000)], is reported.

The Rocket Equation

The Rocket Equation has been known for around one century, having been first contemplated by Tsiolkovski, Oberth and Goddard. It has also been referred to as the mass ratio equation [Bussard and DeLauer (1958), Hill and Petersen (1965)] and the basic Ziolkowsky equation [Lo, (1976)]. The thrust, **F**, that results from expulsion of matter from a vehicle is expressed by Newton's second law, as

$$\mathbf{F} = d(m\mathbf{v}_e)/dt, \qquad (1)$$

where $m\mathbf{v}_e$ is the momentum of the jet exhaust in the vehicle frame of reference, [Corliss, 1960]. For the case where $\mathbf{v}_e$ is constant, differentiation of Equation (1) produces

$$\mathbf{F} = \mathbf{v}_e \, dm/dt. \qquad (2)$$

Figure 1 shows the rocket parameter space based on Equation (2) spanning 14 orders of magnitude in thrust. The power of the rocket jet is $P = \frac{1}{2}\, dm/dt\, v_e^2 = \frac{1}{2}\mathbf{F}v_e$. Specification of any two of the four rocket parameters of interest, (thrust, exit velocity, power, and propellant mass flow rate), fixes the other two parameters. Equation (1) may also be used to define an average exit velocity for rockets where $\mathbf{v}_e$ is not constant, such as blowdown from a fixed volume. Thus, $\mathbf{v}_{e,ave}$ is the total impulse (the integral of **F**dt over the blowdown time) divided by the total mass (the integral of dm over the blowdown time), so that $\mathbf{v}_{e,ave}$ is the mass weighted average exit velocity.

The Rocket Equation results from a balance of the force exerted by the propellant on the vehicle and the motion of the vehicle under the influence of the propulsive force as required by Newton's second law. Thus, in the absence of other forces, such as body (gravitational) force and drag force,

(3) $\mathbf{F} = v_e dm/dt = - mdv/dt.$

where v is the vehicle velocity in the inertial frame of reference, i.e., the velocity relative to a fixed point is space. Elimination of time in Equation (1) yields the expression for conservation of momentum, $mdv = -v_e dm$, which may be integrated between the limits of initial and final mission velocity (v_i and v_f) and mass (m_i and m_f) to produce the Rocket Equation,

(4) $f = m_f/m_i = \exp-(v_f-v_i)/v_e = \exp(-x).$

Mission Efficiencies

The mass, momentum and energy efficiencies for the mission defined by v_f, v_i and v_e follow naturally from the Rocket Equation, viz.,

(5) $\eta_1 = m_f/(m_i-m_f) = f/(1-f) = 1/(e^x-1),$

(6) $\eta_2 = (m_f v_f - m_i v_i)/(m_i-m_f)v_e = f/(1-f)v_f/v_e - 1/(1-f)v_i/v_e = x/(e^x-1) - y,$

(7) $\eta_3 = (m_f v_f^2 - m_i v_i^2)/(m_i-m_f)v_e^2 = f/(1-f)(v_f/v_e)^2 - 1/(1-f)(v_i/v_e)^2 = (x^2+2xy)/(e^x-1) - y^2,$

where $y = v_i/v_e$.

For missions with zero initial velocity, $\eta_1 = 1/(e^x-1)$, $\eta_2 = x/(e^x-1)$, and $\eta_3 = x^2/(e^x-1)$. Figures 2a, 2b, and 2c show three representations of the change in the propulsion efficiencies as the mission progresses from $f = 1$ toward $f = 0$. In the $f = 1$ limit, η_1 is infinite, η_2 is unity, and η_3 is zero. Also, in this limit, $\eta_3 = 1/\eta_1 = x$. When $f = 1/e = 0.367879$, $\eta_1 = \eta_2 = \eta_3 = 0.581976$. A maximum in the energy efficiency, $\eta_3 = 0.647635$, occurs at $f = 0.203179$, $v_f/v_e = 1.59367$. Since these limits are fundamental mathematical constants derived from $e = 2.71828$, they may be written with as many significant figures as desired. The limits may be established by expanding the exponential in a Maclaurin series, viz., $f^1 = e^x = 1 + x + x^2/2! + \ldots$, and truncating after the second term since $x << 1$. The earliest publication of the maximum in η_3, for the case of zero initial velocity, appears to be in Lo's 1976 paper, "Propulsion by laser energy transmission." Phipps, et al. (2000, 2001), optimized their Earth to LEO mission with $v_f/v_e = 1.59367$. The Figures show that the momentum efficiency, initially unity, falls below 0.95 only after the mass fraction decreases below about 0.9. Missions with $f > 0.99$, which includes short Laser Lightcraft flights and bench top measurements of momentum (i.e., impulse, with single laser shots), have $\eta_2 > 0.995$.

Upper stage missions have initial velocities greater than zero. The mass efficiency is independent of the initial velocity, but, as shown in Figure 3a, momentum efficiencies decrease as v_i increases, and, as shown in Figure 3b, energy efficiencies increase as v_i increases. Figure 3b shows that as v_i/v_e increases from zero to unity, the maxima in η_3 increase toward unity and shift toward larger f [or toward smaller $(v_f-v_i)/v_e$]. Thus, the missions of upper stage rockets may be accomplished with higher energy efficiency. For example, if a second stage has a propellant with exit velocity v_{e2} equal to its initial velocity v_{i2}, η_3 is unity when $f = 1$, at the instant of firing the upper stage. As the mission progresses, v increases, f falls below unity, and η_3 falls and eventually becomes negative when $f < 0.0813$. At $f = 0.0813$ the kinetic energy of the vehicle is actually unchanged from what it was at the beginning of the mission but the vehicle velocity is substantially increased to a value around 2.51 times the second stage propellant exit velocity, v_{e2}.

Nearly forty years ago Sutton (1966) introduced the notion of "propulsive efficiency", which we denote η_{Sutton}, to characterize the affect of v_i on the initial value of η_3, i.e., η_{Sutton} = limit as f approaches unity of η_3: $\eta_{Sutton} = y^2/(1-y^2)$ where $y = v_i/v_e$. Sutton described perfect kinetic energy transfer from the jet to the vehicle as the condition achieved when $v_i = v_e$ so that propellant is deposited with zero velocity in the inertial frame of reference.

Coupling Coefficients and Cost Functions

Mass, momentum and energy coupling coefficients (C_1, $\mathbf{C_2}$ and C_3, respectively) indicate the degree of coupling of vehicle parameters to the kinetic energy of the propellant. They are defined as the mass, momentum and energy of the vehicle per unit of propellant kinetic energy, and are simply related to the propulsion efficiencies:

(8) $C_1 = \eta_1/v_e^2$,

(9) $\mathbf{C_2} = 2\,\eta_2/v_e$

(10) $C_3 = \eta_3$

Figure 4 shows the dependence of the momentum coupling coefficient, $\mathbf{C_2}$, on v_e, v_f and f for missions where the initial velocity $v_i = 0$. Figure 4 may be used to show the connection between experimental measurements of $\mathbf{C_2}$ and low altitude flights, where f is near unity, and Earth to LEO missions, where f for maximum energy propulsion efficiency is 0.203. Figure 4 also shows that in the f = 1 limit, $\mathbf{C_2} = 2/v_e$, which is the condition achieved in the experimental work reported here.

The energy coupling coefficient, C_3, and the energy efficiency, η_3, are identical and depend only on the mass fraction and initial velocity as has been previously shown in Figure 3b.

The mission cost functions express mission costs in terms of investment of propellant kinetic energy per unit of vehicle mass, momentum, and energy for a mission specified by v_f, v_i, and v_e. The cost functions are reciprocals of their respective coupling coefficients:

(11) $K_1 = 1/C_1$,

(12) $\mathbf{K_2} = 1/\mathbf{C_2}$,

(13) $K_3 = 1/C_3$.

Phipps, et al. (2000, 2001) used the K_1 cost function (kinetic energy of propellant per unit of propelled mass) in their Earth to LEO mission analysis to illustrate the optimization of mission parameters. The first use of K_1 appears to be in Moeckel's 1976 paper, "Optimum exhaust velocity for laser driven rockets." Figure 5 shows the parameter relationships of K_1 for missions with zero initial velocity. The energy cost is defined as propellant kinetic energy investment per unit of propelled mass. The Figure shows that each mission, specified by v_f, has an optimum v_e, such that K_1 is minimized for $v_f/v_e = 1.5937$. It should be noted however that the minima in K_1 for the lines of constant v_f are quite shallow, and that expenditure of only slightly more energy may be desirable because of the attendant relatively larger gain in mass fraction.

The analysis of a laser powered Earth to LEO mission by Phipps, et al. (2000, 2001) included gravity and drag losses and optimization of mission time to minimize these losses. For their vehicle, they concluded that the required effective v_f was around 10,000 m/s, so that gravity and drag losses amounted to an equivalent velocity loss of about 2,000 m/s over a flight time ~ 800 s. As shown in Figure 4, a propellant with exit velocity of about 6000 m/s and an overall mission momentum coupling coefficient of about 1.2×10^{-4} Ns/J would accomplish the single stage mission to LEO with a mass fraction of 0.203, which translates to propulsion efficiencies of $\eta_1 = 0.255$, $\eta_2 = 0.406$, and $\eta_3 = 0.648$.

Flights of Laser Lightcraft

Knowledge of the momentum coupling coefficient alone, $\mathbf{C_2}$, allows prediction of the altitude as a function of time in short flight experiments. For constant $\mathbf{C_2}$ during the flight, and neglecting drag, the balance of forces on the vehicle of mass M may be written

(14) $\mathbf{F} = M(d^2h/dt^2 - g) = \mathbf{C_2}E_L\omega$,

where h is altitude, ω is laser frequency, and E_L is the energy of one laser pulse incident on the propellant. Equation (14) is appropriate for air, where M remains constant, and for Delrin propellant in flight experiments that utilized very small propellant mass so that M is effectively constant, $f > 0.99$, and $\eta_2 \sim 1$. Integration of Equation (14) from time zero, where $h = 0$, $dh/dt = 0$, $d^2h/dt^2 = 0$, yields altitude as a function of time, coupling coefficient, $\mathbf{C_2}$, laser energy incident on propellant per pulse, E_L, and laser pulse frequency, ω:

$$(15) \qquad h = t^2/2(\mathbf{C_2}E_L\omega/M - g).$$

The thrust to weight ratio alone, T/W, determines the flight characteristics, $T/W = \mathbf{C_2}E_L\omega/Mg$. Since $T/W > 1$, is required for flight, $\mathbf{C_2} > Mg/E_L\omega$ is necessary, where $E_L\omega$ is the effective laser power, P_L. Figure 6 shows predicted flight paths for several values of $\mathbf{C_2}$ that span measured values in single-shot bench top experiments with air and Delrin. The flight paths are shown for a 0.04 kg vehicle propelled by 10 kW of laser power at $\omega = 25$ pulses per second, $E_L = 400$ J/pulse. Figure 7 shows a time exposure photograph of a MLL flight. A new altitude record, $h \sim$ 80 meters was recently achieved with air propellant (Myrabo, October 2000). Obviously, by comparing predicted flight paths to time exposure photography or video tape recordings, coupling coefficients and their variation during the flight may be determined.

Energy Conversion Efficiency of Laser Propulsion

The efficiency of conversion of laser energy to propellant kinetic energy may be defined by energy conservation,

$$(16) \qquad \text{propellant kinetic energy} = \tfrac{1}{2}(m_i\text{-}m_f)v_e^2 = \alpha\beta\, E_L,$$

where E_L is the laser energy incident on the propellant, β is the fraction of energy absorbed into a mass m_i-m_f of propellant, and α is the fraction of the absorbed energy that is converted into propellant kinetic energy by expansion. The value of $\alpha\beta$ may be determined by experimental measurement of the impulse imparted to a test article when a known amount of propellant mass is ejected by a laser pulse of energy E_L. Since

$$(17) \qquad v_e = \mathbf{I}/(m_i\text{-}m_f),$$

$$(18) \qquad \alpha\beta = \mathbf{I}^2/2E_L(m_i\text{-}m_f),$$

which may also be written in terms of the commonly reported experimental coupling coefficient, $\mathbf{C_2(exp)} = \mathbf{I}/E_L$,

$$(19) \qquad \alpha\beta = \mathbf{C_2(exp)}\ \mathbf{I}/2(m_i\text{-}m_f).$$

Thus, to determine $\alpha\beta$, the propellant mass associated with the measured impulse and laser pulse energy must also be measured.

The kinetic energy transferred to a vehicle (in free flight or mounted on a ballistic pendulum) is equivalent to the potential energy it achieves, $m_f gh$. In experiments with $f > 0.999$, this energy is a very small fraction of the total jet kinetic energy, as shown by Equation (7) and Figure 2. However, if the potential energy and propellant mass are measured, a second independent determination of $\alpha\beta$ is possible:

$$(20) \qquad \alpha\beta = (m_i/m_i\text{-}m_f)\ m_f gh/E_L.$$

Thus, two methods for measurement of $\alpha\beta$ are available, both of which require measurement of propellant mass, m_i-m_f. In the impulse measurement, error in the $\alpha\beta$ determination is magnified because $\alpha\beta$ is proportional to $\mathbf{I}^2$, whereas in the potential energy measurement, the $\alpha\beta$ error is proportional to the measured h of a flight experiment or the measured angle of deflection in a ballistic pendulum experiment (*vide infra*).

Experimental

A ballistic pendulum was used to measure the impulse imparted to test articles by absorption of a pulse of laser energy followed by expansion of the heated propellant. The 10 kW pulsed CO_2 laser maintained by the High Energy Laser System Test Facility (HELSTF) at White Sands Missile Range, NM was used. The laser produces pulse energies of 10.6 μm light up to ~ 500 J per pulse over 10 to 30 μs at repetition rates up to about 30 Hz. Laser pulse energy, E_L, was measured with a calorimeter and is accurate to better than 10%.

The three test articles studied were Myrabo Laser Lightcraft (MLL), which is an inverted paraboloid reflector that also acts as a plug nozzle, as illustrated in Figure 8. [see for example, Mead, et al., (2000), Figure 4, for a cross-sectional view]. The focusing optic was identical in each test article. It focused a square beam, ~ 10 cm^2 with a 4 cm^2 central square void, to a circle of laser light that fell on the surface of the aluminum or SiC shroud. With air propellant, the energy is absorbed into a volume of air no larger than ~ 25 cm^3 which, at standard temperature and pressure, amounts to ~ 25 mg of air maximum. This upper limit to the mass of air propellant is based on the geometry of the MLL model 200-3/4 geometry. With Delrin propellant, the mass of ablated propellant was determined by weighing before and after each series of ablation experiments at fixed E_L. Table I summarizes the test article masses, pendulum total masses, m_{pen} and distances, l, between the pivot and center of gravity.

Table I. Experimental test articles and pendulum parameters, MLL model 200-3/4.

article	article mass, kg	pendulum mass, m_{pen}, kg	c of g, l, m	propellant
bare pendulum	0.7035113	0.7035113	0.3556	
1. heavyweight model, aluminum shroud	0.3140756	1.0175869	0.3826	air
2. SiC shroud flight model	0.1141644	0.8176757	0.3683	air
3. SAR (solid ablative rocket) flight model	0.1241798	0.8276911	0.3690	Delrin plus air

The experimental impulse was obtained from the measured maximum angle of deflection, θ, of the pendulum during the first half cycle after imparting the impulse:

$$(21) \qquad I = m_{pen}[gl(1-\cos\theta)]^{1/2} \sim m_{pen}\pi\theta\,[gl]^{1/2}/720,$$

where m_{pen} is the pendulum plus test article mass, g is the gravitational constant, 9.806 m s^{-2}, and l is the distance between pendulum pivot and center of gravity [Thomas (1953)]. The approximation to Equation (21), which derives from the Maclaurin expansion for cosθ, is accurate to better than one part in ten thousand when $\theta < 10$ degrees. Equation (21) derives from the equivalence between the initial kinetic energy and the potential energy when the pendulum is at maximum deflection, $\frac{1}{2} m_{pen}v_{pen}^2 = m_{pen}gl(1-\cos\theta)$ under conditions where there are no losses. Based on the measured damping, the energy loss was about 0.00015 J (0.6 %) per half-cycle of the total of 0.0230 J of potential energy when the largest value of θ, ~ 7 degrees, was measured so no correction for this loss was made to the data.

The mass of propellant was typically a few tens of milligrams, which amounts to a mass fraction of f ~ 0.9999 to 0.99999. Thus, whereas momentum from the jet is transferred to the pendulum with unit efficiency, $\eta_2 = 1$, the energy of the jet is transferred to the pendulum with efficiency $\eta_3 \sim 10^{-4}$ to 10^{-5} (see Figure 2).

For each of the test articles, the pendulum was calibrated with an NBS traceable impulse hammer. The hammer imparted impulses ranging from 0.005 to 0.04 N-s in about 15 ms. Figure 9 compares the impulse from the hammer calibrations to those obtained from the pendulum. The figure shows that the ratio, $I_{pendulum}/I_{hammer}$, varied within about 2 % of unity, and indicates that $I_{pendulum}$ is systematically higher. This is probably due to a small energy loss in the hammer calibration that occurs during the imperfect impact of the hammer against the pendulum.

Results

Figure 10 shows the mass of Delrin ablated, m_D, as a function of E_L for the SAR test article, and Figure 11 shows the exit velocity based on the measured impulse, $v_e = I/m_D$. Since a small amount of air could also become involved in the propellant expansion, the v_e values represented here are upper limits. m_D was measured to an accuracy of a few tenths of milligrams by difference weighing with a Mettler balance.

Figure 12 shows the dependence of the overall energy conversion efficiency, $\alpha\beta$, on E_L for the SAR test article. Since these values of $\alpha\beta$ are based on the measured impulse, they do not account for possibly significant pendulum losses that may occur when the laser thrust profile [a few hundred microseconds long, (Jones, 2001)] is imposed on the Lightcraft. These losses are nearly absent in the hammer calibrations where the thrust profile is stretched over a one hundred fold longer time scale. The high instantaneous thrust of the laser initiated detonation may lead to significant loss in the somewhat loose moving parts of our ballistic pendulum. If these losses were quantified $\alpha\beta$ would increase. It should be pointed out that this series of pendulum measurements was immediately followed by identical experiments where impulse was measured with a fast piezo electric transducer capable of better than 1 ms time resolution. The piezo electric measurements (Jones, 2001) showed that the integrated impulse were nearly two times the impulse measured with the pendulum. This means, since $\alpha\beta$ goes as the square of the impulse, that $\alpha\beta$ may be significantly larger than has been derived here from pendulum measurements without consideration of losses.

Figure 13 summarizes selected momentum coupling coefficients, C_2, obtained for air and Delrin propellants over the course of several experimental test periods at WSMR during the past few years with our ballistic pendulum. There appears to be a strong dependence of C_2 on the quality of the beam, as between a tightly focused beam that produces lower C_2 with air propellant than a loosely focused beam. This may be due to the tight beam heating a smaller mass of air to a higher energy than the more diffuse loosely focused beam. Although the exit velocity is higher in the tight beam case, the total impulse is lower because the heated mass is lower. Comparison of air to Delrin propellant with a tightly focused beam shows that with Delrin the measured C_2 values are two to three times larger, probably because a larger mass of Delrin is ablated than is heated in the case of air.

Discussion of Thermodynamic Considerations

Figure 14 shows the chemical equilibrium Mollier diagram for air up to 24,000 K. Figure 14 is based on the database maintained at NASA/Glenn (McBride and Gordon (1996) which is certified accurate up to 20,000 K and based on extended 9-parameter fits to enthalpy, heat capacity, and entropy of neutral species and singly charged ions. Above 20,000 K doubly charged ions begin to contribute but these are not included in the database.

In Figures 15 and 16 we show an abbreviated pair of Mollier diagrams for air which we use to illustrate process representations of conversion of internal energy to kinetic energy and to compare this energy conversion when isentropic expansions occur under conditions of equilibrium (Figure 15) or frozen flow (Figure 16). This is a highly simplified, single parameter analysis based on the notion of an absorption volume into which a fraction, β, of the incident laser energy is deposited. Thus, we may consider the range of internal energy appropriate for the model 200-3/4 MLL that would be applicable to laser heated air in our experiments. The Figures show a scale of specific internal energy with $\beta = 1$ based on the three conceivable volumes of laser heated air at STP density (1.18 kg/m^3), 5.4, 21.7, and 43.4 cm^3. These are the volumes of toroids with 0.5, 1.0, and 1.5 cm diameters that fit snugly into the shroud of the model 200-3/4 MLL. The scales show that a specific internal energy of 4e7 J/kg would be reached when about 260 J of laser energy is deposited into 5.4 cm^3 or when about 1000 J of laser energy is deposited into 21.7 cm^3 of STP air. Additionally, the state with specific internal energy of 2e7 J/kg would be reached with about 120 J deposited in 5.4 cm^3 or about 500 J in 21.7 cm^3 of STP air. The Figures also show three isentropes originating from the constant u = 4e7 J/kg line and the constant u = 2e7 J/kg line. These isentropes are labeled wih circles that indicate the area ratios for the isentropic expansion.

Figure 15 shows that equilibrium blowdown from the 4e7 J/kg, 1.18 kg/m^3 state with an area ratio of 4 produces an exit pressure of ~ 1 atm and exit internal energy, $u_e \sim 2.8e7$. The exit velocity is thus $v_e = [2(4e7-2.8e7)J/kg]^{1/2} = 4900$ m/s and the fraction of energy converted to kinetic energy is $\alpha = 1.2e7/4e7 = 0.3$. In comparison, blowdown from the 2e7 J/kg, 1.18 kg/m^3 state with an area ratio of 4 also produces an exit pressure of ~

1 atm and the exit internal energy, $u_e \sim 1.2e7$. The exit velocity is thus $v_e = [2(2e7-1.2e7)J/kg]^{1/2} = 4000$ m/s and the fraction of energy converted to kinetic energy is $\alpha = 0.8e7/2e7 = 0.4$. Thus, the indications are that laser heating to higher internal energy results in lower energy conversion efficiency but higher exit velocity.

Comparison of frozen blowdown (Figure 16) shows that frozen flow loss occurs. With area ratio of 4, from the u = 4e7 J/kg, $\rho = 1.18$ kg/m^3 initial state, $v_e = 4500$ m/s and $\alpha = 0.22$ (loss of ~ 400 m/s in v_e and 0.08 in α), and from the u = 2e7 J/kg state, $v_e = 3200$ m/s and $\alpha = 0.25$ (loss of 800 m/s in v_e and 0.15 in α). Comparison of Figures 15 and 16 shows that frozen losses increase drastically when the effective area ratio increases beyond 4.

Figure 17 shows the dependence of α on area ratio and initial density for isentropic blowdown from u = 4e7 J/kg to an exit pressure determined by the area ratio. In Figure 17 only the energy conversion from momentum thrust is captured. At area ratio of 4 the exit pressure is ~ 1 atm. With an initial density of STP air (1.18 kg/m^3) the Figure shows $\alpha = 0.31$. In Figure 18 the efficiency of energy conversion from both momentum and pressure thrust by blowdown to vacuum is shown. Similarly, for u = 4e7 J/kg, area ratio of 4, initial density of STP air, the Figure shows $\alpha = 0.40$, so that operation in vacuum produces a substantial (~ 25%) increase in the conversion of internal energy to propellant kinetic energy.

Figure 19 shows exit velocity from equilibrium expansion of air heated to u = 4e7 J/kg and initial densities ranging from 1e-5 to 1e2 kg/m^3 as a function of area ratio. Curves with filled triangles denote exit velocity that derives from momentum thrust alone and are transformations of isentropes from the Mollier plane that originate from the constant u = 4e7 J/kg line. Curves defined by squares show exit velocity for expansion into vacuum and include impulse from momentum and pressure thrust. Curves defined by circles show exit velocity for expansion to 1 atm external pressure. These are truncated at the point where the impulse from pressure thrust becomes negative due to over-expansion of the propellant for the given area ratio. The actual average exit velocity from the blowdown beginning at a given density is the density weighted average exit velocity. For example, the heavy solid line represents the vacuum exit velocity for blowdown from an initial density of 1 kg/m^3 and an area ratio of 4. Initially the exit velocity is ~ 5800 m/s and the nozzle exit density is ~ 0.09 kg/m^3. After 90% of the propellant has blown down, the exit velocity is ~ 5500 m/s and the nozzle exit density is ~ 0.009 kg/m^3. After 99% blowdown, the exit velocity is ~ 5300 m/s and the nozzle exit density is ~ 0.0009 kg/m^3. At 99.9% blowdown exit velocity is 5100 m/s and the nozzle exit density is 0.0.00009 kg/m^3. Thus the average vacuum exit velocity is ~ 5763 m/s, is only ~ 1% less than the initial exit velocity. In this example, if expansion to external pressure of 1 atm pressure at area ratio of 4 is considered, the initial exit velocity is 5500 m/s and after 90% blowdown it is ~ 5000 m/s. Thus, there is a significant negative pressure thrust involved when blowdown to 1 atm external pressure occurs.

Conclusions

Experimental studies of the 200-3/4 model Myrabo Laser Lightcraft with air and Delrin propellants heated by 10.6 m radiation from a CO2 laser showed that energy conversion efficiencies of laser energy to propellant kinetic energy were at least 30% and may be as high as 50%. This was found to be consistent with highly simplified analysis of the thermodynamics of equilibrium from initial states specified by a single parameter, the volume into which the laser energy is absorbed. The measured exit velocity based on measured Delrin mass and estimated air mass are in the neighborhood of ~ 2000 – 3000 m/s, which is somewhat less than predicted by the thermodynamic model. In the case of Delrin, it was noted that laser pulse energies in excess of ~ 350 J/pulse frequently caused fragmentation and ejection of large macro chunks of propellant ~ 500 mg, when clean ablation produced only about 30 mg of propellant. The relatively low exit velocity measured in the case of Delrin, ~ 2000 m/s, is quite probably due to the ablation of a significant fraction material as molecules or assemblies of molecules in addition to hydrogen and carbon monoxide. It should be noted that beam quality plays an important role in the performance of the model 200-3/4 MLL which is counterintuitive inasmuch as lower beam quality (energy spread over a larger area) produces higher C_2 coupling coefficients in the bench top and flight experiments of the past. Computational fluid dynamics modeling of the absorption (and reflection) of laser energy and expansion of the formed plasma [Wang, Chen, Liu, Myrabo, and Mead (2001)] have recently been carried out. The simple analysis presented here may only be useful in providing upper limitations to the conversion of laser energy to propellant kinetic energy and to provide a simplified visualization and description of the processes occurring in blowdown of laser heated propellants in MLL devices.

Bibliography

1. Bussard, R. W., and DeLauer, R. D., "Nuclear Rocket Propulsion," McGraw Hill, New York, 1958.
2. Corliss, William R., "Propulsion Systems for Space Flight," McGraw-Hill Book Company, 1960.
3. Hill, Philip G., and Peterson, Carl R., "Mechanics and Thermodynamics of Propulsion," Addison-Wesley Publishing Company, London, 1965.
4. Jones, Jonathan, to be published (2001), personal communications.
5. Liu, Jiwen, Chen, Yen-Sen, and Wang, Ten-See, "Accurate prediction of radiative heat transfer in laser induced air plasmas," 34th AIAA Thermophysics Conference, 19-22 June 2000, Denver, CO, paper 2000-2370.
6. Lo, R. E., "Propulsion by laser energy transmission (considerations to selected problems)," IAF PAPER 76-165, October 1, 1976, 11 pages.
7. Lo, R. E., "Rocket engines as energy converters of extremely high power density," Astronautik, Volume 12, Issue 2, Page 27-31, January 1, 1975. In German. Maximum energy conversion efficiency of 64.76 % and deltaV/Vexit = 1.5936. Abstract states "parameter study is diagramed."
8. Lo, R. E., "Raketentriebwerke als Energiewandler extrem hoher Leistungsdichte,"Vortrag auf dem 23. Raumfahrtkongreß der Hermann-Oberth-Ges. e.V., Salzburg, 27.6.1974 und Astronautik, Heft 2, Jg. 12 (1975), S. 27-31, 6 Bilder, 1 Tabelle
9. Lo, R. E., "Propulsion by Laser Energy Transmission (Considerations to Selected Problems)." 27. IAF-Kongress, Anaheim, Cal., 12.10.1976, Preprint IAF-76-165, 1976, 10 p, 12 Figs, 3 Tables
10. McBride, Bonnie J., and Gordon, Sanford, "Computer program for calculation of complex chemical equilibrium compositions and applications, II. Users manual and program description," NASA Reference Publication 1311, Lewis Research Center, Cleveland, OH 44135, June 1996.
11. Mead, Franklin B. Jr., Squires, Stephen, Beairsto, Chris, and Thurston, Mike, "Flights of a laser-powered Lightcraft during laser beam hand-off experiments," 36th AIAA Joint Propulsion Conference, 16-19 July, Huntsville, AL, paper 2000-3484.
12. Messitt, Donald G., Myrabo, Leik N. and Mead, Franklin B. Jr., "Laser initiated blast wave for launch vehicle propulsion," 36th AIAA Joint Propulsion Conference, 16-19 July, Huntsville, AL, paper 2000-3035.
13. Moeckel, W. E., "Optimum exhaust velocity for laser-driven rockets," J. Spacecraft, Vol. 12, No. 11, Pages 700-701, manuscript received May 12, 1975, revision received July 11, 1975. Shows derivation of deltaV/Vexit = 1.5936.
14. Myrabo, L. N., press release, "New altitude record achieved by Laser Lightcraft at White Sands Missile Range, October 9, 2000, (October 2000).
15. Phipps, C. R, Reilly, J. P., and Campbell, J. W., "Optimum parameters for laser-launching objects into low earth orbit," *Lasers and Particle Beams*, **19**(1), in press (2001).
16. Phipps, C. R, Reilly, J. P., and Campbell, J. W., "Laser launching a 5-kg object into low earth orbit," Presented at the Third International Symposium on High Power Laser Ablation, Santa Fe, NM, 23-28 April 2000, *Proceedings of SPIE* **4065**, 502 (2000).
17. SEA Software, Inc., "Thermo-Chemical Equilibrium Program (TEP)," Carson City, NV, 1999.
18. Sutton, George P., "Rocket Propulsion Elements," John Wiley & Sons, Inc, New York, 1992.
19. Thomas, William T., "Mechanical Vibrations," Prentice-Hall, Inc., Englewood Cliffs, NJ, 1953.
20. Wang, Ten-See, Chen, Yen-Sen, Liu, Jiwen, Myrabo, Leik N., and Mead, Franklin B. Jr., "Advanced Performance Modeling of Experimental Laser Lightcrafts," 39th AIAA Aerospace Sciences Meeting and Exhibit, 8-11 January 2001, Reno, NV, Paper 2001-0648.

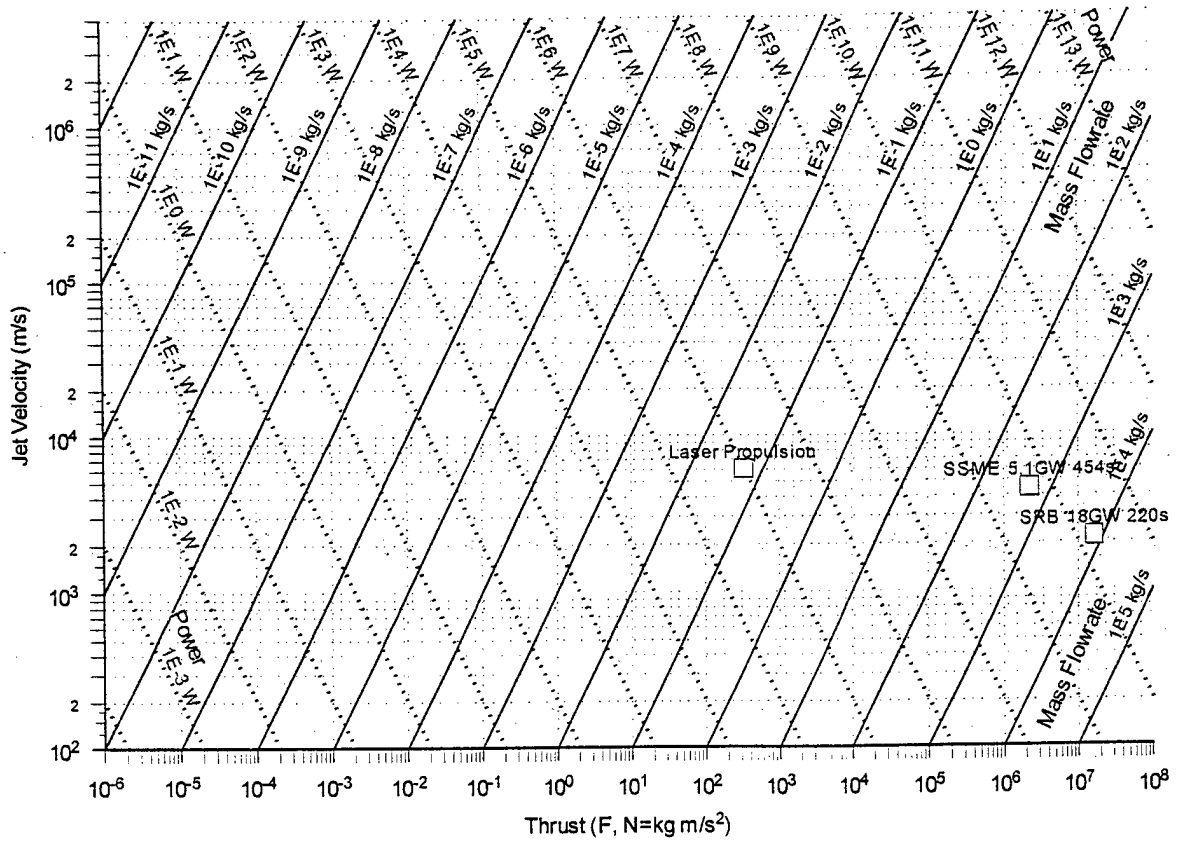

Figure 1. Parameter space for rockets: $F = v_e\, dm/dt$, and P (power) = ½ $dm/dt\, v_e^2$.

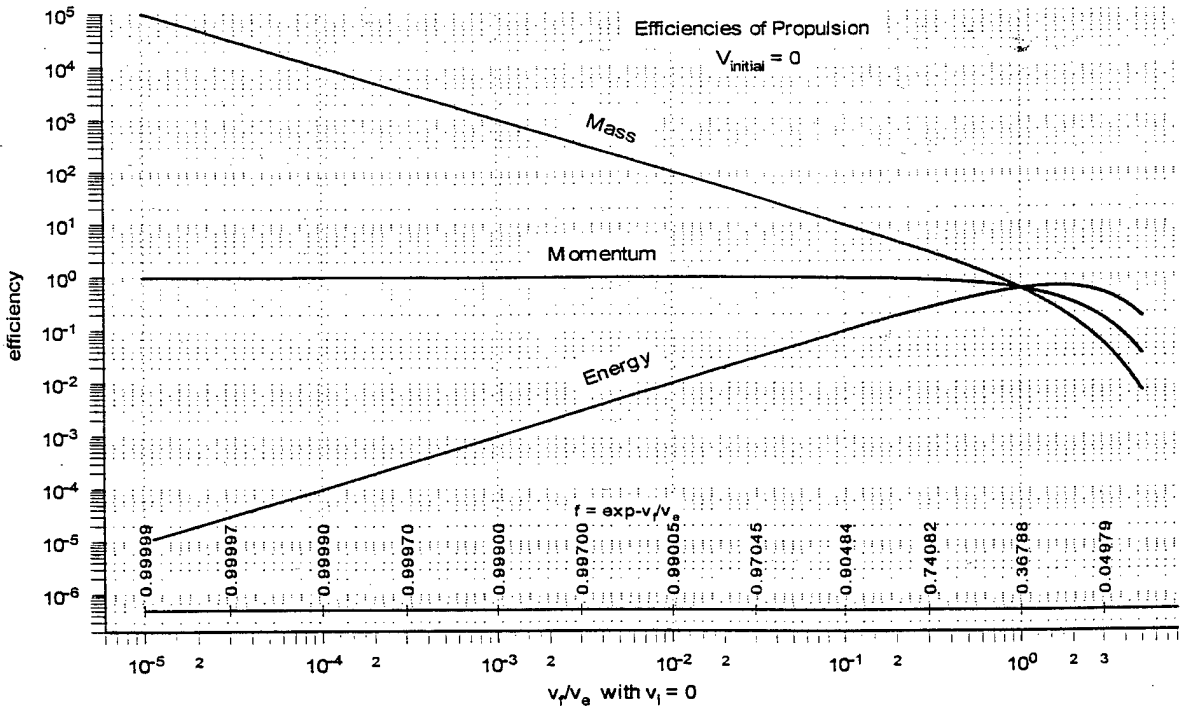

Figure 2a. Propulsion efficiencies for missions with zero initial velocity.

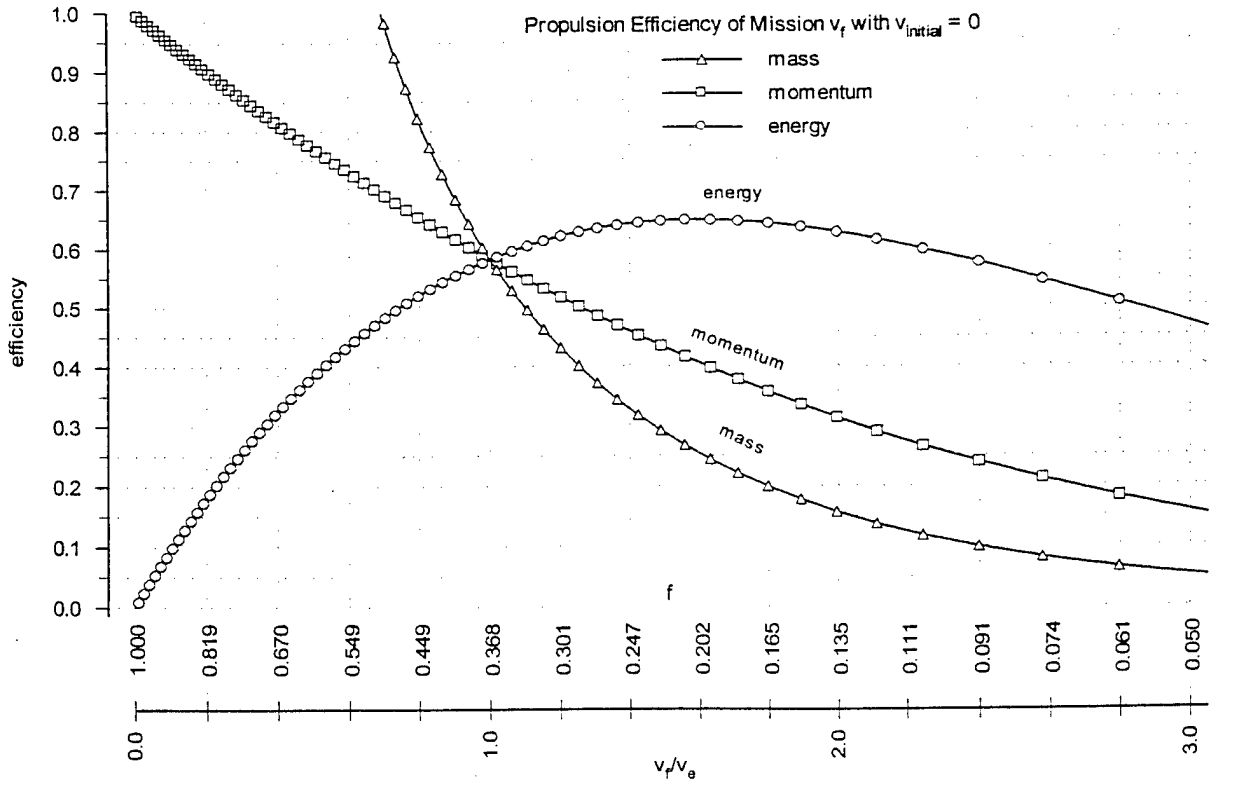

Figure 2b. Propulsion efficiencies for missions with zero initial velocity, linear in v_f/v_e.

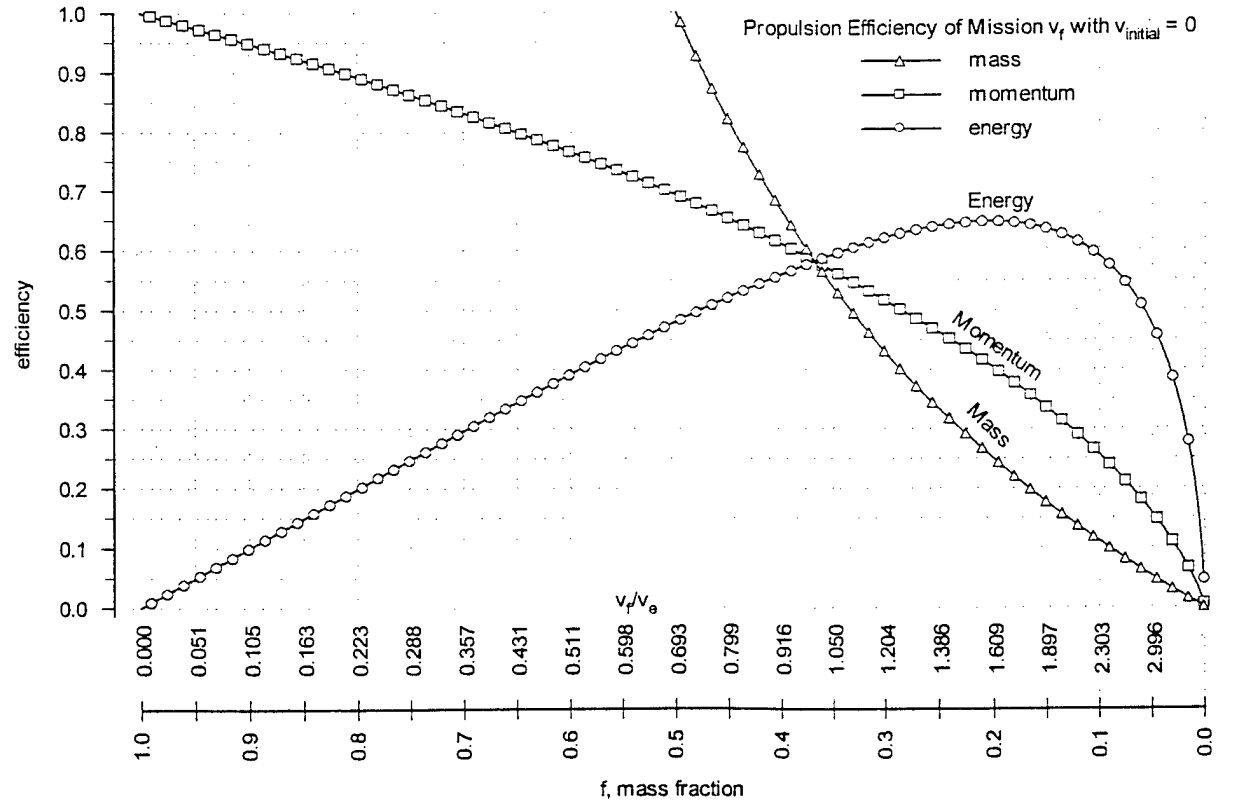

Figure 2c. Propulsion efficiencies for missions with zero initial velocity, linear in f.

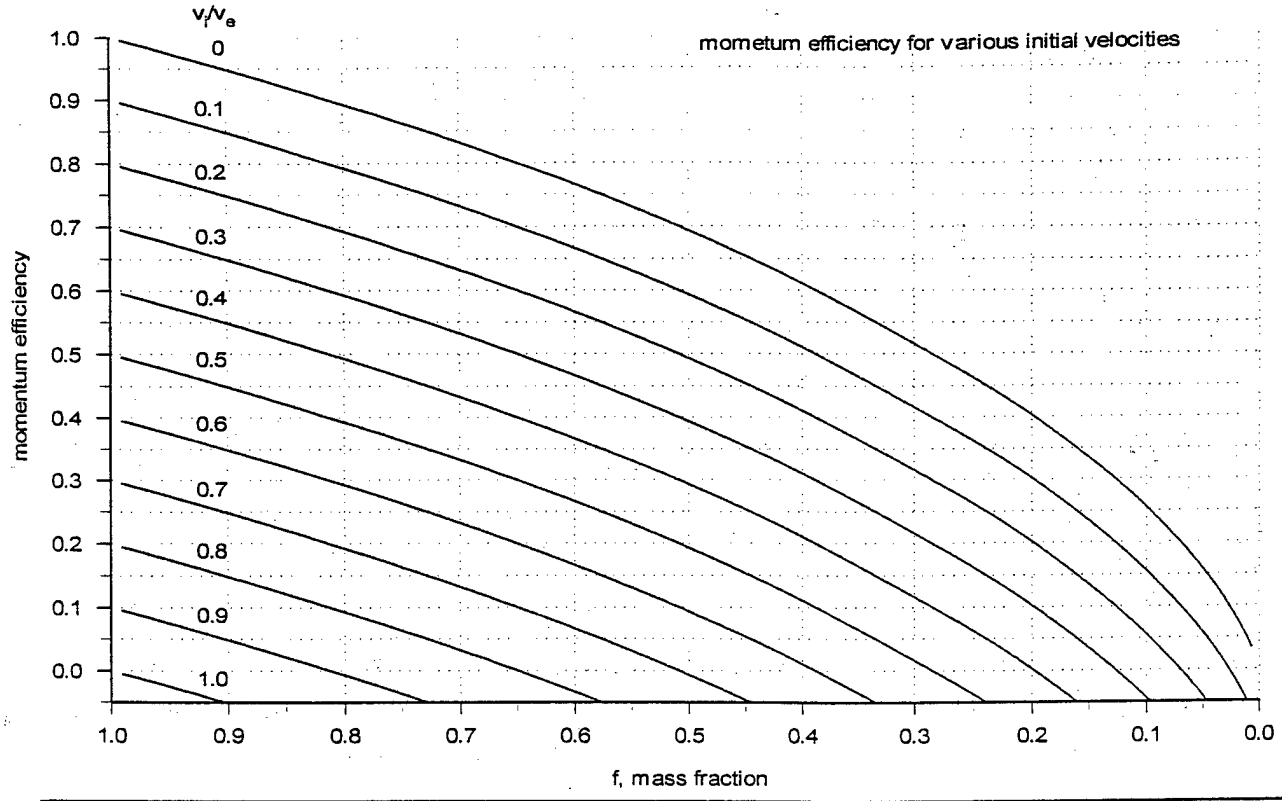

Figure 3a. Momentum efficiency for missions with various initial velocity, v_f/v_e = 0 to 1.

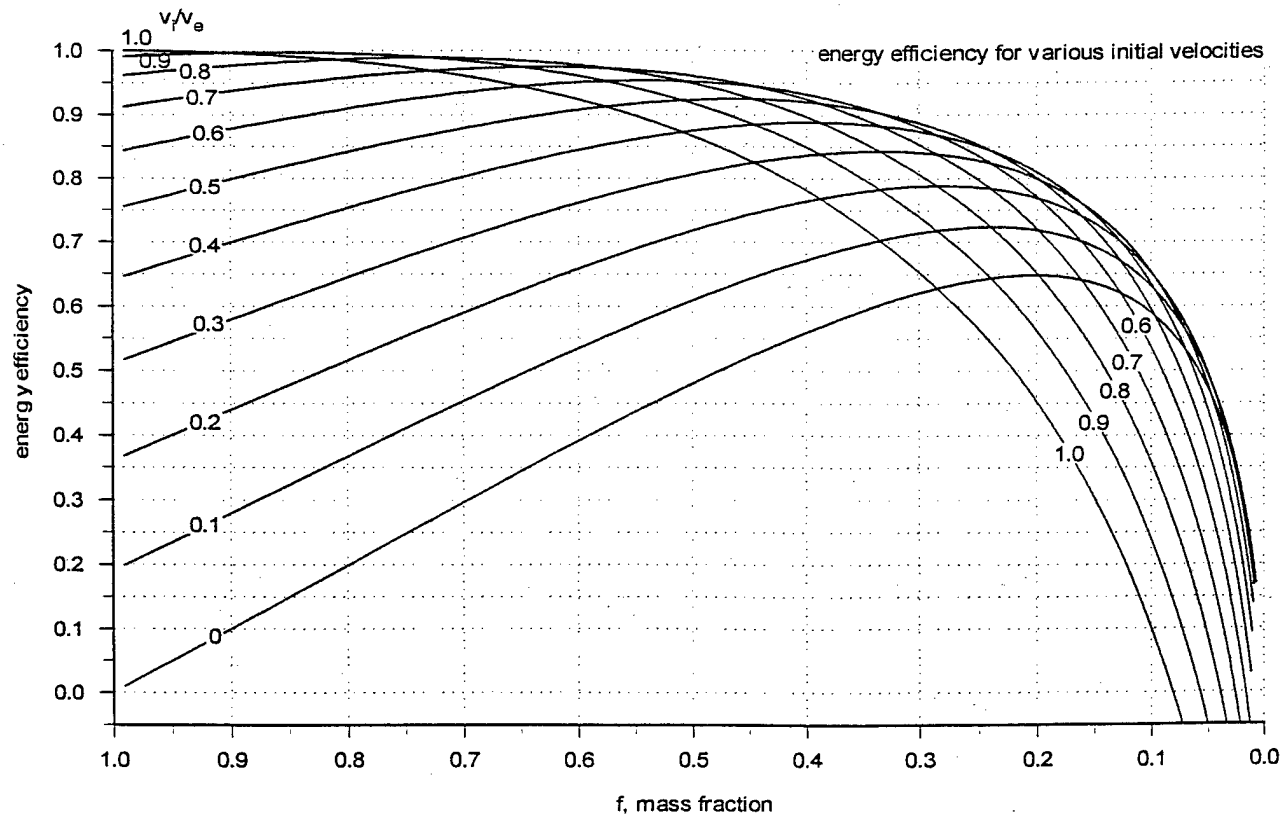

Figure 3b. Energy efficiencies for missions with various initial velocity, v_f/v_e = 0 to 1.

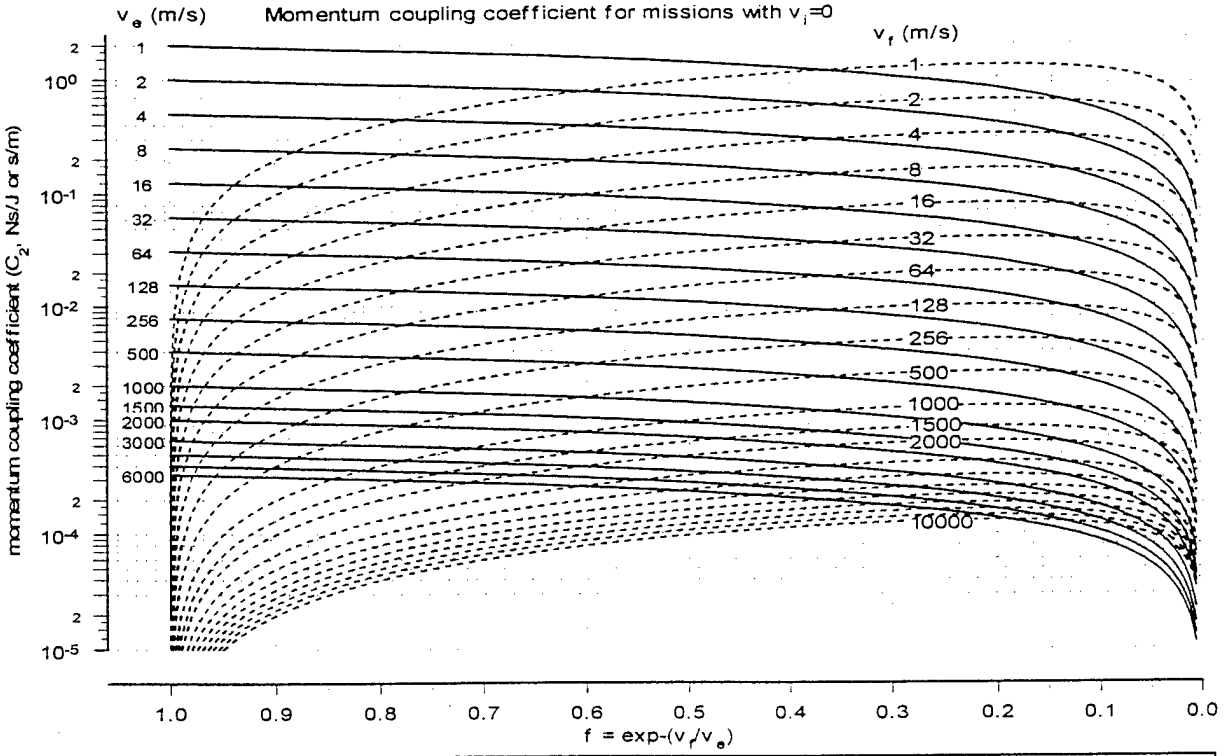

Figure 4. Momentum coupling coefficient for missions with zero initial velocity as a function of v_e, v_f, and f. Lines of constant v_f (dotted lines) and v_e (solid lines) are shown at increments of 1000 m/s above 2000 ms. In the limit of $f = 1$, $C_2 = 2/v_e$. The Earth to LEO mission requires $v_f \sim 10{,}000$ m/s including gravity and drag losses, which is optimized at $f \sim 0.2$ with $v_e = 6000$ m/s and $C_2 \sim 0.0001$ Ns/J [Phipps, Reilly and Campbell (2000)].

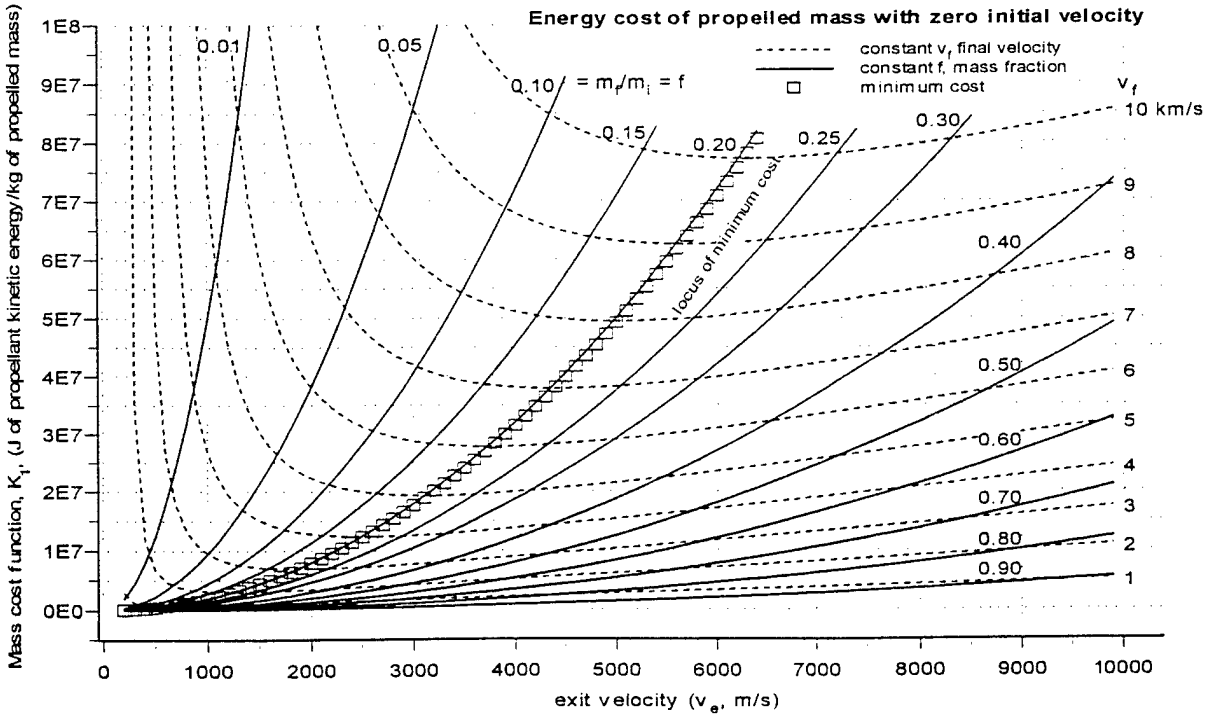

Figure 5. Mass cost function, K_1, as used by Phipps, Reilly and Campbell (2000) in Earth to LEO mission analysis. The value of K_1 is optimized for all missions with zero initial velocity when $f = 0.203$.

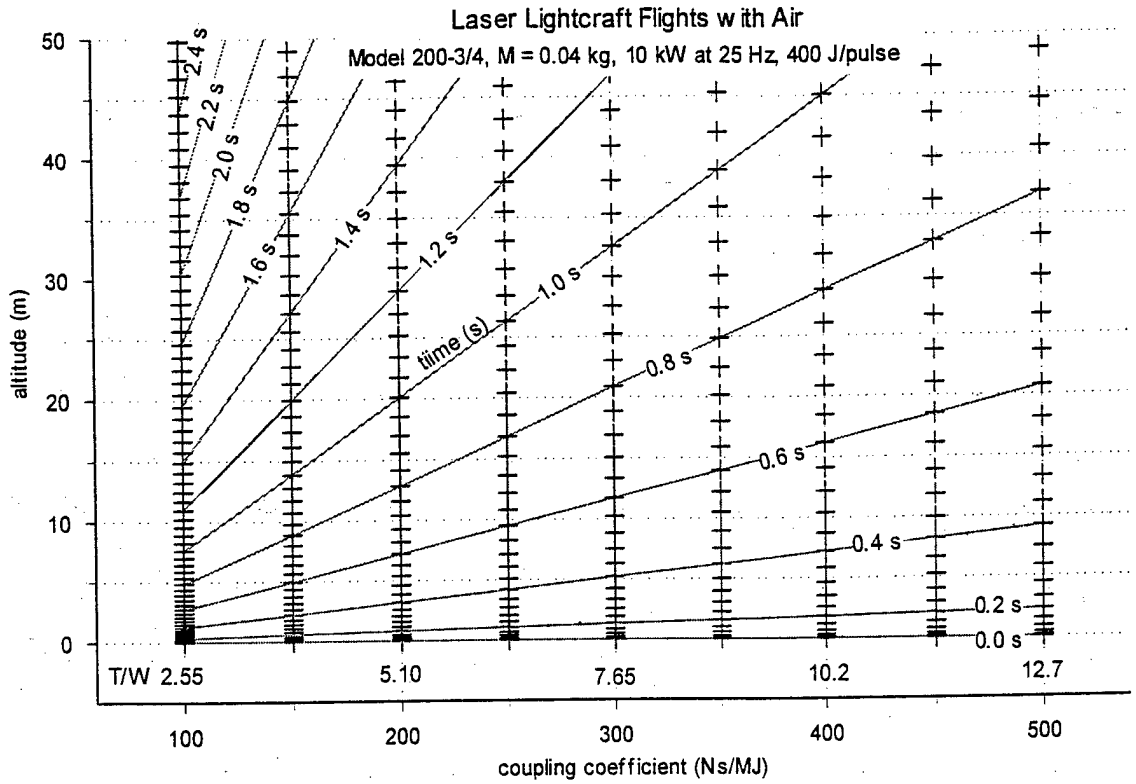

Figure 6. Laser Lightcraft flights with air with various coupling coefficients for a Model 200-3/4 laser Lightcraft, with mass of 40 grams. These flight patterns are also valid for flights with onboard propellant provided that the mass of ablated propellant is much less than the test article mass, $f > 0.99$. T/W = 1 when $C_2 = 39.2$ Ns/MJ.

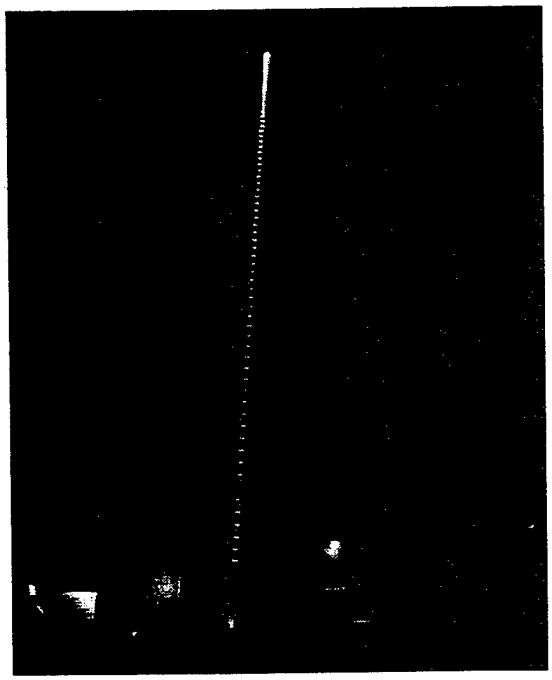

Figure 7. Time exposure of nighttime flight of Myrabo Laser Lightcraft. The time between flashes of the air plasma is 0.04 s.

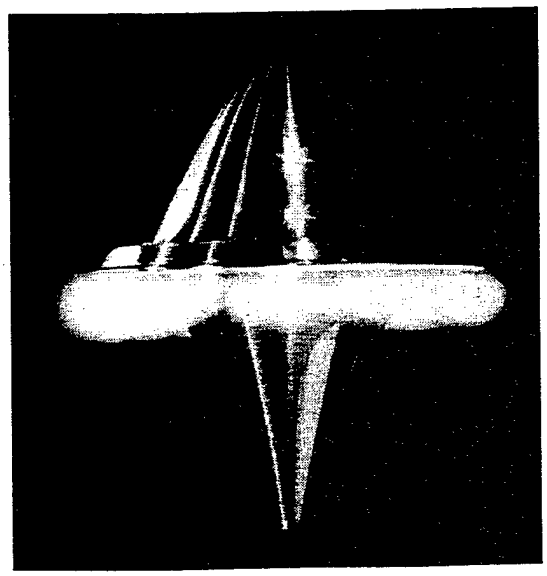

Figure 8. The Myrabo Laser Lightcraft showing air plasma. The Model 200-3/4 is ~ 0.1 m diameter at largest circumference. The aluminum model weighs ~ 30 g without Delrin. About 10 g of Delrin was used in the Solid Ablative Rocket (SAR) of which ~0.3 g was ablated during a typical flight with about 100 shots.

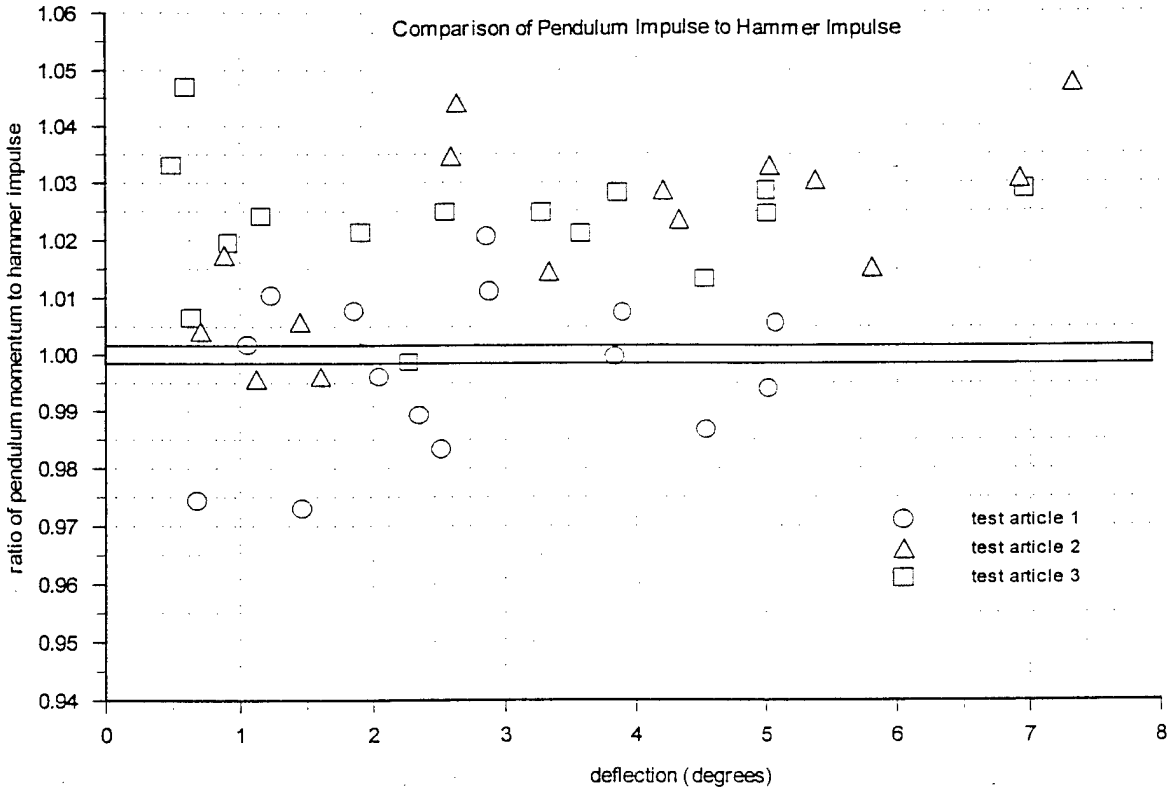

Figure 9. Comparison of Impulse measured by ballistic pendulum to impulse measured with standard hammer accelerometer.

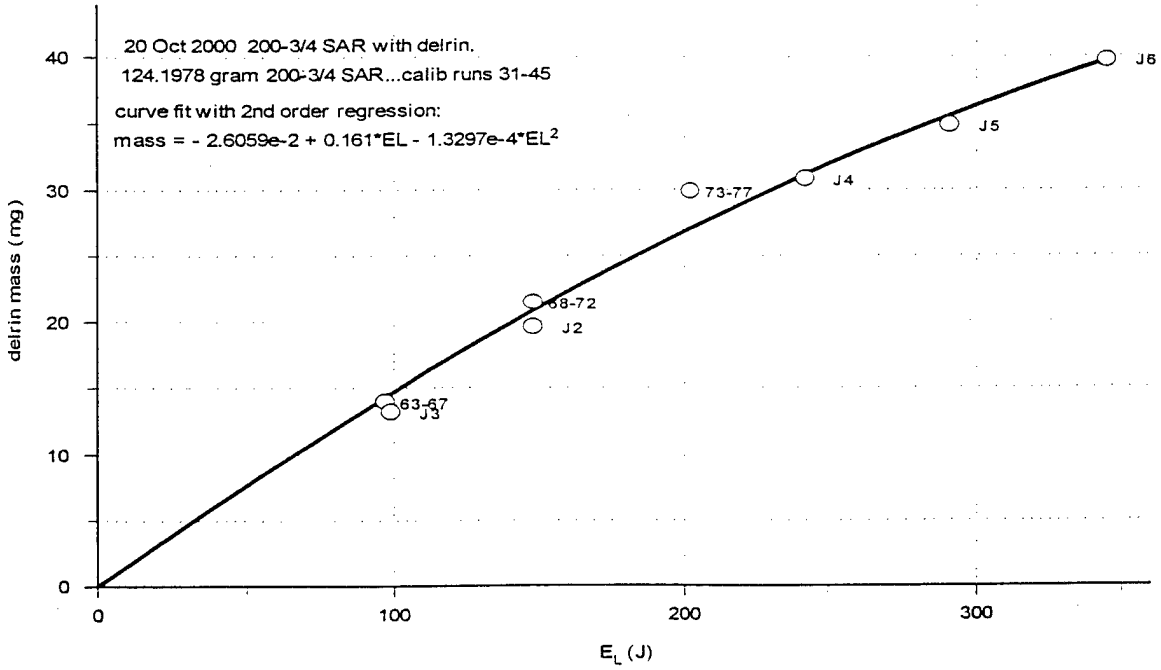

Figure 10. Mass of Delrin evaporated per laser pulse of given energy. The points labeled with a 'J' were accompanied by impulse measurements with a piezoelectric transducer which indicated that the duration of the thrust was applied over a time of several hundred microseconds (Jones, 2001). The width of the laser pulse was ~ 18 us.

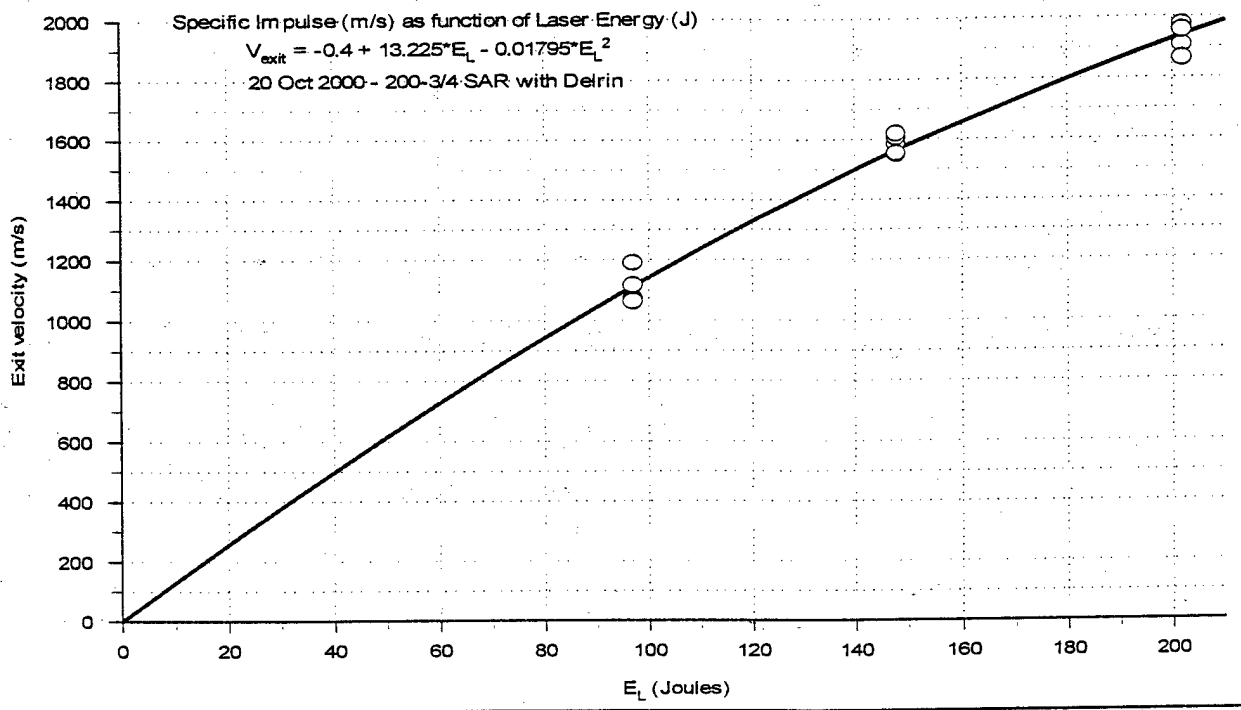

Figure 11. Exit velocity of Delrin based on measured impulse and measured mass of ablated Delrin.

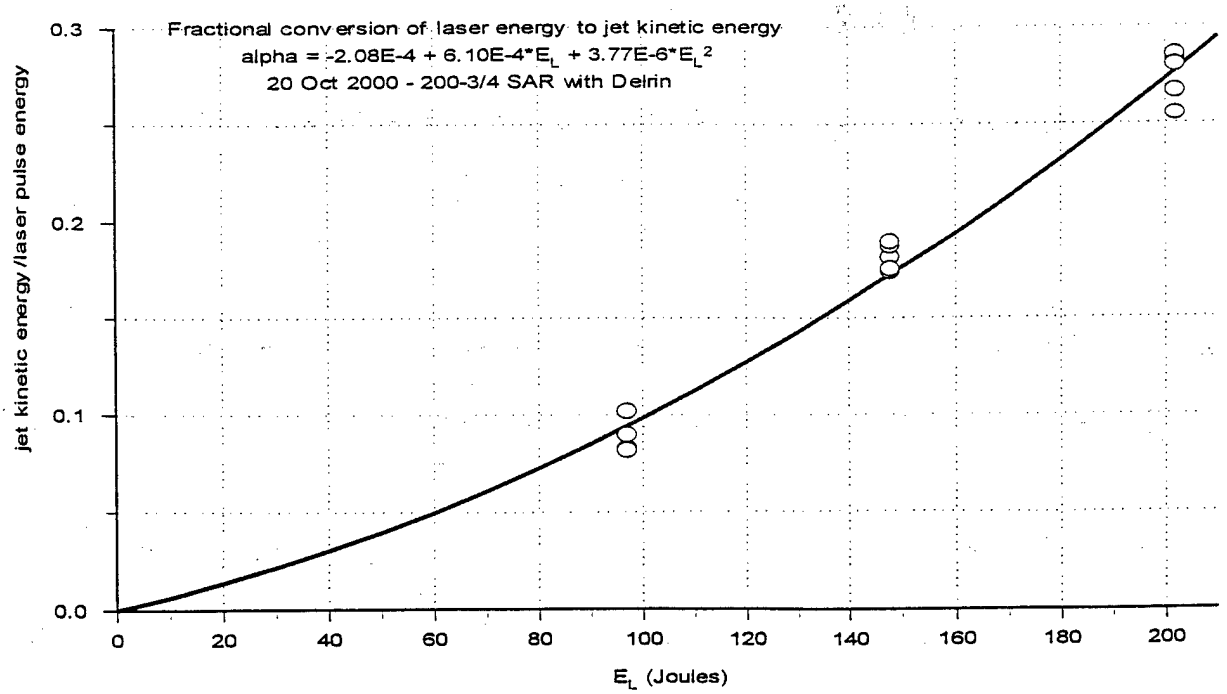

Figure 12. Fractional conversion of laser energy to propellant kinetic energy ($\alpha\beta$) with Delrin propellant.

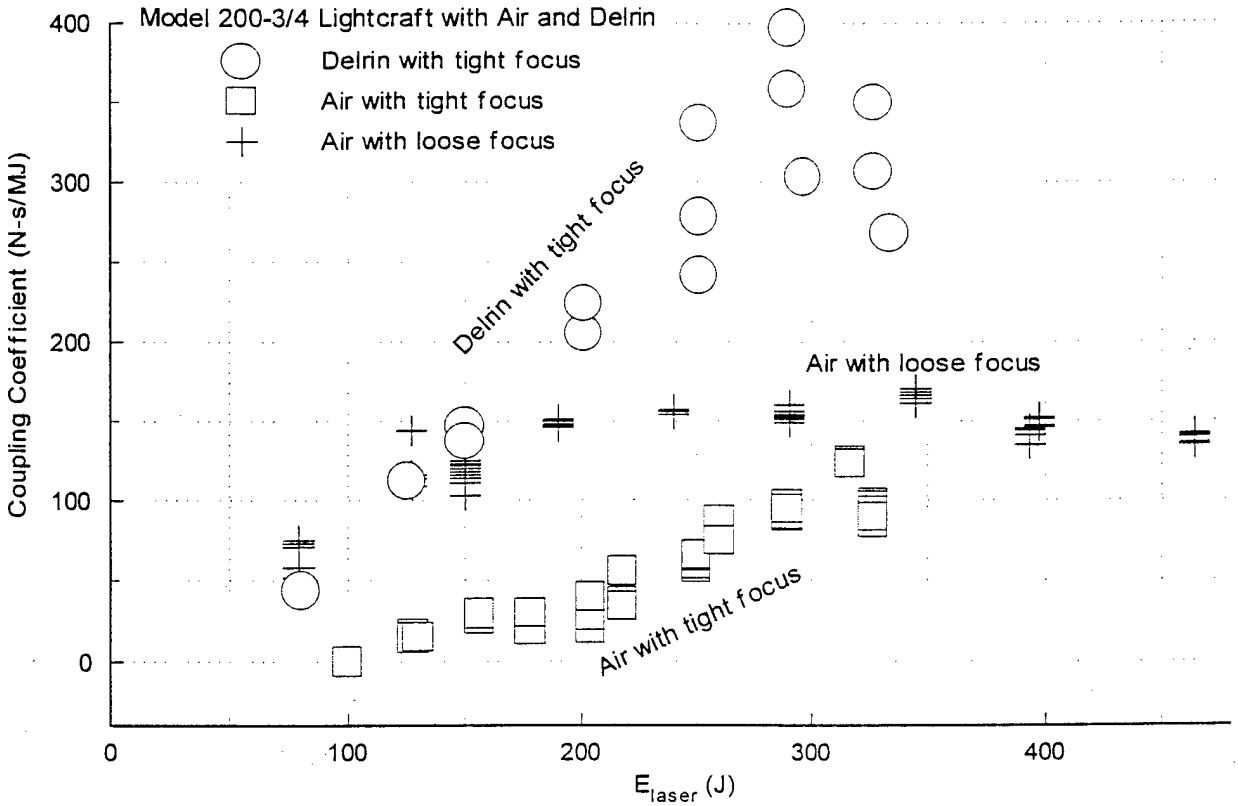

Figure 13. Comparison of coupling coefficient measured for air and Delrin with a tightly focused laser beam and comparison of tightly focused and loosely focused laser beam with air propellant. The lower quality beam produced a higher coupling coefficient and Delrin produced about three times higher coupling coefficient than air

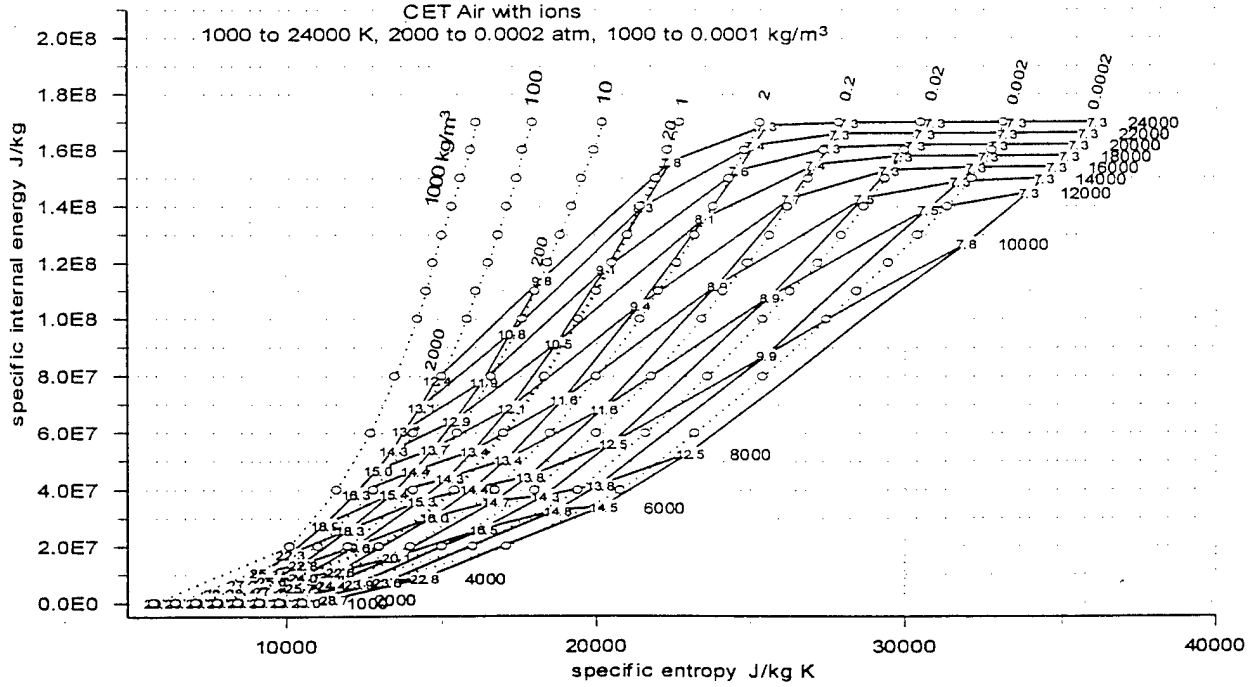

Figure 14. Mollier diagram for air including singly ionized species derived from NASA/GLENN Chemical Equilibrium Applications [McBride and Gordon (1996)] database. Constant density lines are indicated by circles connected with dotted lines. Molecular weight is indicated at intersections of isobars and isotherms. The 1996 database is certified accurate up to 20,000 K. At 20,000 K air is fully ionized below ~ 1 atm.

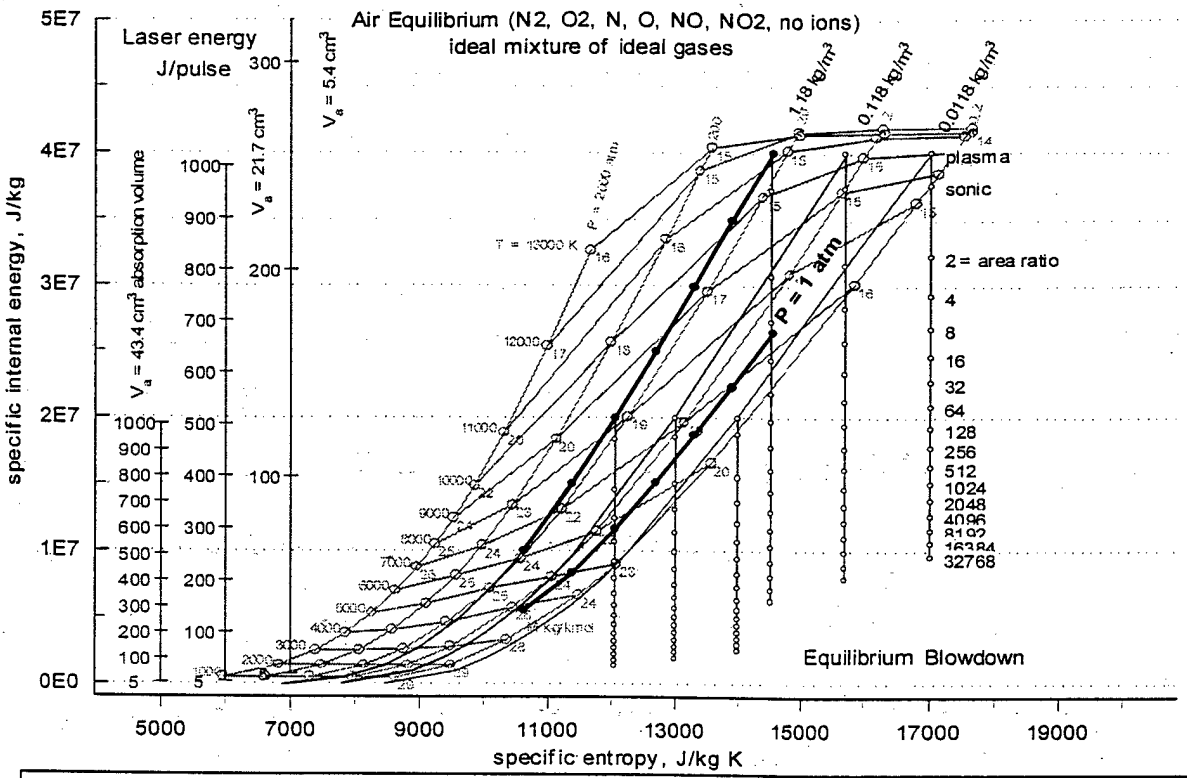

Figure 15. Mollier diagram for equilibrium air without ions. Numbers adjacent to intersections of isobars and isotherms indicate average molecular weight. Upper heavy line is a constant density = 1.18 kg/m^3 line. three isentropes from u = 4e7 and 2e7 J/kg represent equilibrium blowdown for the indicated area ratios, 1 to 32768. The P = 1 atm isobar is reached with an area ratio ~ 8 from the initial u = 4e7 and ~ 4 from the u = 2e7 J/kg state, respectively. The exit velocities from these two expansions are ~ 5000 and 3000 m/s, respectively.

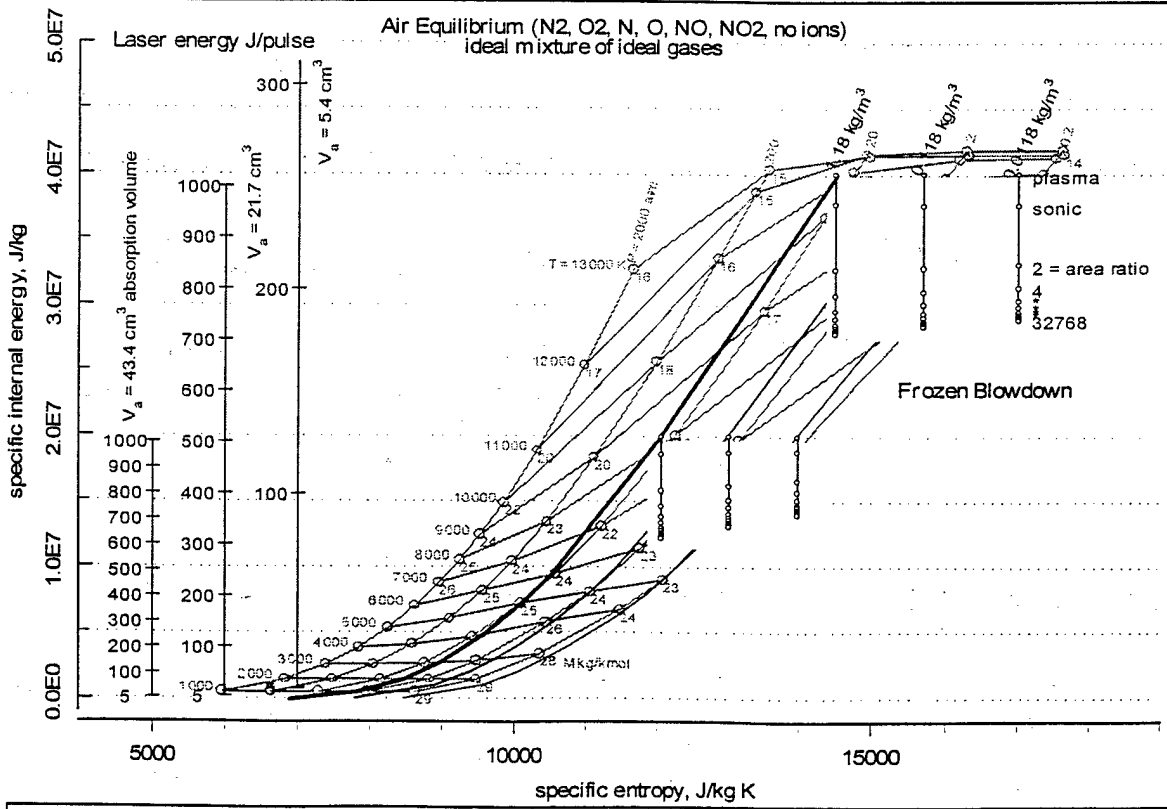

Figure 16. Process representations of air expansion with frozen blowdown, as in Figure 15. The frozen isentropic expansions from u = 4e7 and 2e7 J/kg and 1.18 kg/m3 to 1 atm produce exit velocities of 5000 and 3000 m/s, only slightly less than the equilibrium expansions represented in Figure 15.

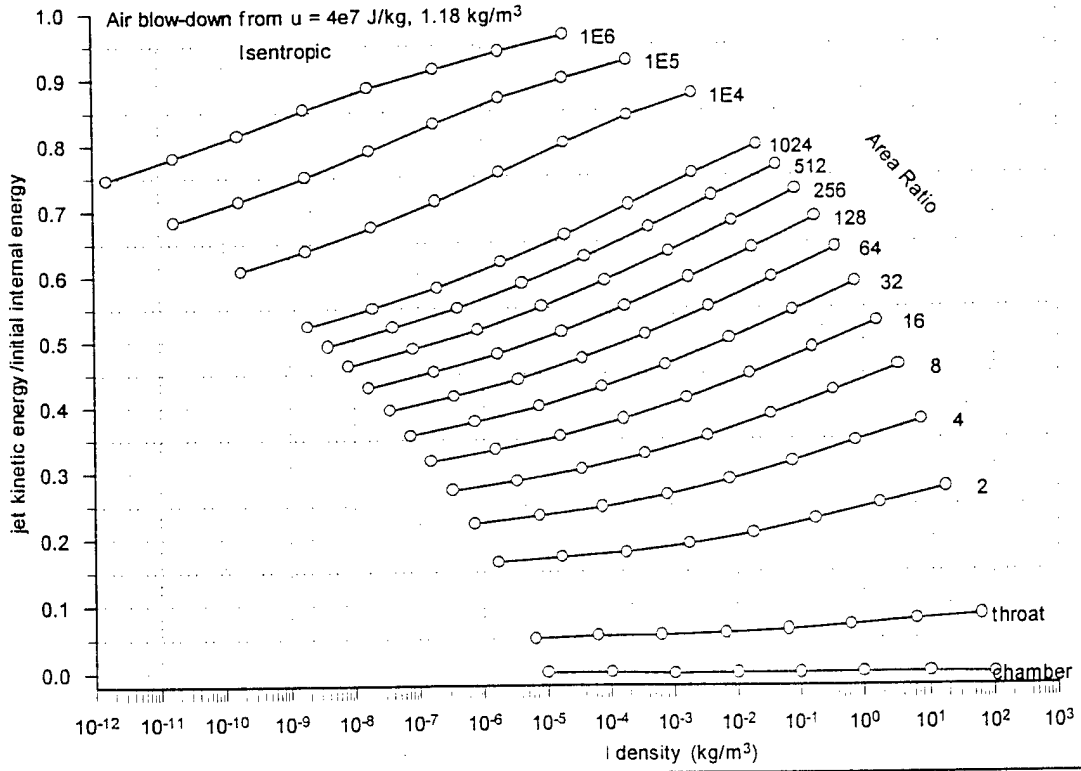

Figure 17. Fractional energy conversion ($\alpha\beta$) as a function of initial density and area ratio for isentropic blowdown of air heated to specific internal energy 4e7 J/kg. For initial density of 1 kg/m[3] and an area ratio of 4, $\alpha\beta$ = 0.35. $\alpha\beta$ values, calculated for equilibrium expansion, are only a few % larger than frozen expansion.

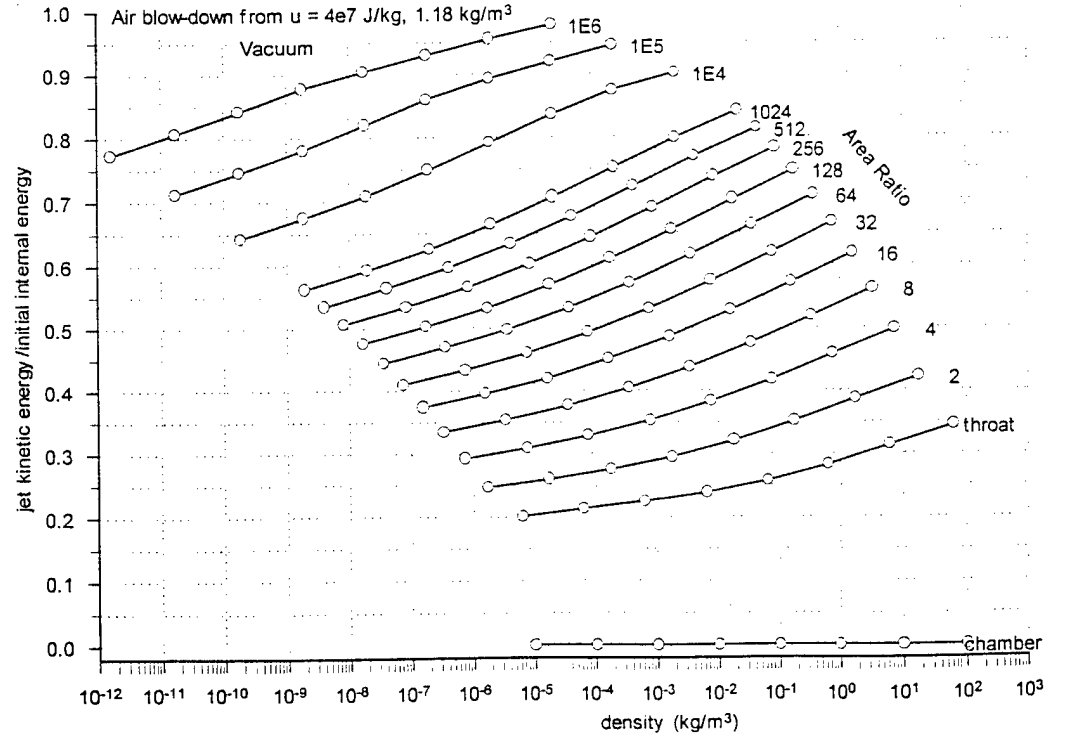

Figure 18. Fractional energy conversion ($\alpha\beta$) as a function of initial density and area ratio for blowdown of air heated to specific internal energy 4e7 J/kg and expanded to vacuum. For initial density of 1 kg/m^3, $\alpha\beta$ = 0.50 for an area ratio of 4. $\alpha\beta$ values, calculated for equilibrium expansion, are only a few % larger than frozen expansion.

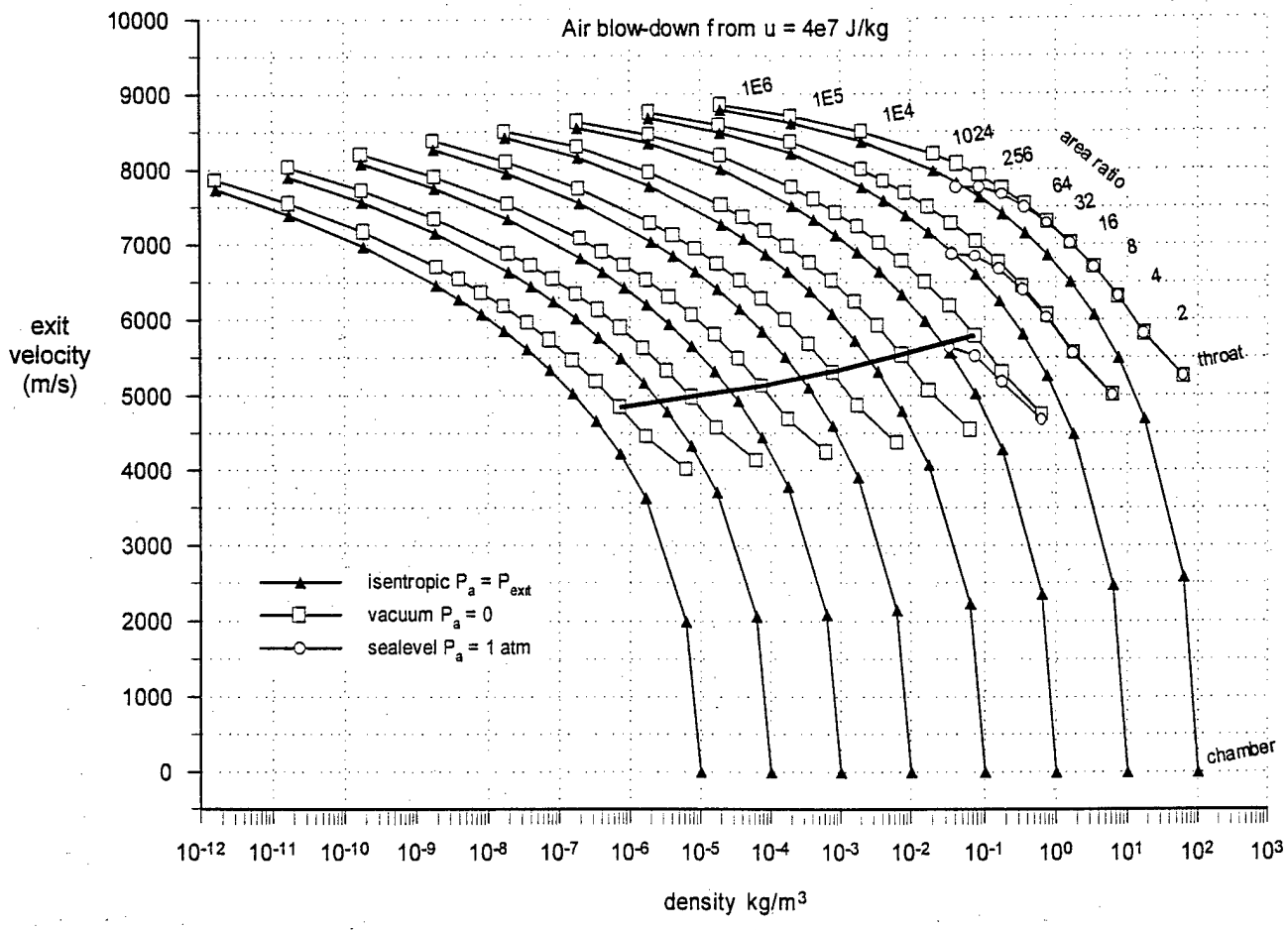

Figure 19. Exit velocity from equilibrium expansion of air heated to u = 4e7 J/kg and initial densities ranging from 1e-5 to 1e2 kg/m^3 as a function of area ratio. Curves with filled triangles denote exit velocity that derives from momentum thrust alone and are transformations of isentropes from the Mollier plane that originate from the constant u = 4e7 J/kg line. Curves defined by squares show exit velocity for expansion into vacuum and include impulse from momentum and pressure thrust. Curves defined by circles show exit velocity for expansion to 1 atm external pressure. These are truncated at the point where the impulse from pressure thrust becomes negative due to over expansion of the propellant for the given area ratio. The actual average exit velocity from the blowdown beginning at a given density is the density weighted average exit velocity. For example, the heavy solid line represents the vacuum exit velocity for blowdown from an initial density of 1 kg/m^3 and an area ratio of 4. Initially the exit velocity is ~ 5800 m/s and the nozzle exit density is ~ 0.09 kg/m^3. After 90% of the propellant has blown down, the exit velocity is ~ 5500 m/s and the nozzle exit density is ~ 0.009 kg/m^3. After 99% blowdown, the exit velocity is ~ 5300 m/s and the nozzle exit density is ~ 0.0009 kg/m^3. At 99.9% blowdown exit velocity is 5100 m/s and the nozzle exit density is 0.0.00009 kg/m^3. Thus the average vacuum exit velocity is ~ 5763 m/s, is only ~ 1% less than the initial exit velocity. In this example, if expansion to external pressure of 1 atm pressure at area ratio of 4 is considered, the initial exit velocity is 5500 m/s and after 90% blowdown it is ~ 5000 m/s. Thus, there is a significant negative pressure thrust involved when blowdown to 1 atm external pressure occurs.